

LLNL-JRNL-401466



LAWRENCE
LIVERMORE
NATIONAL
LABORATORY

Molecular Dynamics Simulations of Temperature Equilibration in Dense Hydrogen

J. Glosli, F. Graziani, R. More, M. Murillo, F. Streit, M.
Surh, L. Benedict, S. Hau-Riege, A. Langdon, R.
London

February 19, 2008

Physical Review ERapid Communications

Disclaimer

This document was prepared as an account of work sponsored by an agency of the United States government. Neither the United States government nor Lawrence Livermore National Security, LLC, nor any of their employees makes any warranty, expressed or implied, or assumes any legal liability or responsibility for the accuracy, completeness, or usefulness of any information, apparatus, product, or process disclosed, or represents that its use would not infringe privately owned rights. Reference herein to any specific commercial product, process, or service by trade name, trademark, manufacturer, or otherwise does not necessarily constitute or imply its endorsement, recommendation, or favoring by the United States government or Lawrence Livermore National Security, LLC. The views and opinions of authors expressed herein do not necessarily state or reflect those of the United States government or Lawrence Livermore National Security, LLC, and shall not be used for advertising or product endorsement purposes.

Molecular Dynamics Simulations of Temperature Equilibration in Dense Hydrogen

J. N. Glosli,¹ F. R. Graziani,¹ R. M. More,¹ M. S. Murillo,² F. H. Streitz,¹
M. P. Surh,¹ L. X. Benedict,¹ S. Hau-Riege,¹ A. B. Langdon,¹ and R. A. London¹

¹*Lawrence Livermore National Laboratory*

²*Los Alamos National Laboratory*

(Dated: February 10, 2008; Received)

The temperature equilibration rate in dense hydrogen (for both $T_i > T_e$ and $T_i < T_e$) has been calculated with large-scale molecular dynamics simulations for temperatures between 10 and 300 eV and densities between $10^{20}/cc$ to $10^{24}/cc$. Careful attention has been devoted to convergence of the simulations, including the role of semiclassical potentials. We find that for Coulomb logarithms $\mathcal{L} \gtrsim 1$, Brown-Preston-Singleton [Brown et al., Phys. Rep. **410**, 237 (2005)] with the sub-leading corrections and the fit of Gericke-Murillo-Schlages [Gericke et al., PRE 65, 036418 (2003)] to the T-matrix evaluation of the collision operator, agrees with the MD data to within the error bars of the simulation. For more strongly-coupled plasmas where $\mathcal{L} \lesssim 1$, our numerical results are consistent with the fit of Gericke-Murillo-Schlages.

I. INTRODUCTION

In high energy density plasmas relevant to Inertial Confinement Fusion (ICF) capsules, thermonuclear burn depends on the energy exchange between the particles making up the plasma. The ability to accurately simulate thermonuclear burning plasmas using a radiation-hydrodynamic code depends on knowing the electron-ion energy exchange due to Coulomb collisions. The reason is the strong temperature dependence of thermonuclear reaction rates. A small change in the electron-ion energy exchange affects the ion temperature and hence the transient burn characteristics of the plasma. Unfortunately, complexity of the theoretical models and the limitations of the existing experimental data means that electron-ion coupling models are an important source of uncertainty in ICF calculations. The experimental data that does exist comes from non-equilibrium plasmas generated using either lasers or shocks. To date, these experiments are very indirect and limited to the cool side of the warm dense matter regime, which is dominated by Fermi degeneracy [1]. Ongoing experiments at the OMEGA laser and planned experiments on NIF will investigate the two temperature equilibration problem for dense high energy density plasmas undergoing thermonuclear burn. But, until then, data is still lacking. The purpose of this paper is to describe a complementary approach using an N-body simulation of hot, dense plasmas based on molecular dynamics techniques. We use this method to test the theoretical models most commonly implemented in ICF codes.

The theoretical electron-ion energy exchange depends on the coupling rate ($1/\tau_{ie}$) which can be written in the form,

$$\frac{1}{\tau_{ie}} = \frac{8\sqrt{2\pi}n_i(Ze^2)^2}{3m_em_ic^3} \left\{ \frac{kT_e}{m_e c^2} + \frac{kT_i}{m_i c^2} \right\}^{-3/2} \mathcal{L} \equiv \frac{\mathcal{L}}{J_{LS}} \quad (1)$$

J_{LS} is defined as the Landau-Spitzer pre-factor and \mathcal{L} is a dimensionless function defined below. n_i and n_e are the

ion and electron number densities, Z is the ion charge, and T_e and T_i are the electron and ion temperatures. The dimensionless function \mathcal{L} incorporates correlated collisions peculiar to the Coulomb potential. That is, small impact parameters are associated with strong collisions and large impact parameters are associated with collective phenomena. The electron-ion coupling rate was first calculated for classical plasmas by Landau [2] and Spitzer (LS) [3] in the approximation of small angle scattering. The small angle scattering assumption has been relaxed in subsequent classical treatments by including exact (hyperbolic) particle trajectories (HLS) [4].

For weakly coupled plasmas obeying (1) Full ionization (2) No radiation (3) Static Debye screening, \mathcal{L} takes on a simple form. The LS formula uses two ad hoc cutoffs, one for short distances and the other for long distances while the hyperbolic orbit calculation requires a cutoff only at long distances. The Landau-Spitzer calculations yield the so-called Coulomb logarithm $\mathcal{L}_{LS} = \ln b_{\max}/b_{\min}$ and the subsequent modification due to hyperbolic orbits yields

$$\mathcal{L}_{HLS} = .5 \ln \left(1 + \left(\frac{b_{\max}}{b_C} \right)^2 \right) \quad (2)$$

b_{\max} is chosen to be the Debye length $\lambda_D = \sqrt{kT_e/4\pi e^2 n_e}$ and for LS models, b_{\min} is chosen to be the classical distance of closest approach ($b_C = Ze^2/kT$). At short distances, where quantum diffraction effects are expected to play a role, the short distance scale is assumed to be some combination of b_{\min} and the electron thermal deBroglie wavelength $\Lambda = \sqrt{2\pi\hbar^2/m_e kT_e}$.

The presence of ad hoc cutoffs led to numerous works devoted to a rigorous derivation of kinetic equations without cut-offs, called Convergent Kinetic Theories (CKT). Frieman and Book [5], Gould and DeWitt [6], and recently Gericke, Murillo and Schlages (GMS) [7] have applied these ideas to dense plasma temperature equilibration. They investigated the various physics approximations going into an evaluation of \mathcal{L} , including LS, HLS and concluding with a quantum kinetic approach. For the latter case, GMS define an effective Coulomb logarithm

\mathcal{L}_{GMS} that best agrees with the T-matrix evaluation of the collision operator for static screening and the one they recommend as the best model,

$$\mathcal{L}_{GMS} = .5 \ln \left(1 + [\lambda_D^2 + R_{ion}^2] / [\Lambda^2 / 8\pi + b_C^2] \right) \quad (3)$$

Where $R_{ion} = (3/4\pi n_i)^{1/3}$ is the ion sphere radius. We will refer to this model as GMS-T to emphasize the T-matrix connection.

Recently, Brown, Preston and Singleton [8] and Brown and Singleton [9] used dimensional regularization to obtain an expression for the electron-ion coupling rate valid for fully ionized weakly coupled plasmas for non-degenerate and degenerate electrons, respectively. Their method gives both leading and sub-leading contributions to \mathcal{L} , namely, for non-degenerate electrons,

$$\mathcal{L}_{BPS} = \log(\lambda_{Debye}/\Lambda) + (\log(16\pi) - \gamma - 1) / 2 \quad (4)$$

(γ is the Euler constant).

The most direct method of studying temperature equilibration is with numerical simulations that include strong, collective scattering at all length scales; this is the forte of molecular dynamics (MD) methods. Hansen and McDonald (HM) [10] explored dense hydrogen temperature equilibration using MD, and found MD results in excellent agreement with the LS approach, with a Coulomb logarithm given by $\log(\lambda_{Debye}/\Lambda)$. Because MD solves the exact classical equations of motion for the N-body system, this agreement is persuasive. However, the HM simulations were performed with (1) a small number of particles ($N = 128$), (2) no ensemble averaging, and (3) no assessment of the sensitivity to the effective semi-classical potential that was used to prevent 3-body recombination. Here, we employ MD methods that remove these constraints and find that for $\mathcal{L} \gtrsim 1$, both BPS and GMS-T agree with the MD data to within the error bars of the simulation. For $\mathcal{L} \lesssim 1$, the MD simulations are consistent with GMS-T except for the coldest, degenerate cases.

II. MOLECULAR DYNAMICS: SIMULATION AND RESULTS

Simulations are applied to a neutral system of protons and electrons in a cubic cell with periodic boundary conditions. The MD is performed using a basic leapfrog method in a massively parallel implementation [11]; the Coulomb interaction is incorporated by an Ewald summation [12]. We adjust the timestep, Δt , to conserve total energy over the entire simulation ($\Delta E/E < 10^{-4}$) and avoid distorting the calculated relaxation rate. Typical Δt values range from 5×10^{-5} to 10^{-3} fs. Energy drift is important in such simulations because artificial heating can spoil the determination of the true relaxation rate.

Convergence with respect to particle number is tested by employing various particles numbers N ranging from $N = 128$ (the number that HM employed), to as many as $N = 64,000$. Finally, sensitivity to the initial conditions is determined by choosing several equivalent members of an ensemble for each case. The nonequilibrium system is prepared using two separate Langevin thermostats for protons and electrons. Initial configurations are sampled from a stationary distribution obtained after up to $10^6 - 10^7$ timesteps. The thermostats are then removed, and the species allowed to undergo collisional relaxation. Sensitivity to initial conditions is studied by sampling multiple, independent systems from a microcanonical ensemble and/or by discarding a portion of the initial temperature evolution.

Most runs are long enough to extract a relaxation time (typically 10% of τ_{pe}), with some of the strong-coupling cases continued to complete equilibration. From fitting the temperature derivatives over a brief interval, and using:

$$\frac{dT_e}{dt} = \frac{T_p - T_e}{\tau_{ep}} \quad (5)$$

$$\frac{dT_p}{dt} = \frac{T_e - T_p}{\tau_{pe}} \quad (6)$$

we obtain τ_{pe} . Temperature relaxation is asymmetric in the strong-coupling cases (in contrast to the energy flow), but $|dT_e/dt|$ and $|dT_p/dt|$ differ by only about 10% and therefore we consider only τ_{pe} .

The above expression assumes an ideal gas equation of state for the plasma. For strongly coupled plasmas, there is a potential energy contribution to the energy exchange rate which would imply that the energy exchange rate is no longer described by equations (5) and (6). However, as Gericke and Murillo show [13], the error associated with using the temperature evolution equations is small in the temperature-density regimes of interest here.

Because the classical Coulomb many-body problem is unstable for attractive interactions, we employ semi-classical effective potentials [14] that prevent the unphysical formation of deeply bound states. The potentials reduce the Coulomb interaction on short length scales, which is consistent with the use of the thermal deBroglie wavelength for b_{min} in Landau-Spitzer approaches. The forms chosen were also used by HM, viz. the Dunn and Broyles [15] plus Deutsch potentials [16].

$$V_{ab}^{DB}(r) = \frac{Z_a Z_b e^2}{r} \left(1 - \exp \left(-\sqrt{2\pi} r / \Lambda_{ab} \right) \right) \quad (7)$$

The thermal deBroglie wavelengths are $\Lambda_{ab} = \sqrt{2\pi\hbar^2/\mu_{ab}T}$ where μ_{ab} is the reduced mass and $T = T_e$ except when a and b are both ions and $T = T_i$. The expressions are temperature-dependent, but the parameters are held fixed in the simulations rather than using the fluctuating MD values. The calculated relaxation rates

Case	$n_i(1/cc)$	$T_e(eV)$	$T_i(eV)$	$n_e\Lambda^3$	Γ	$\tau_{pe}^{sim}/2 (fs)$	$\sigma(fs)$
A	10^{20}	10.0	20.0	10^{-3}	.1	2.10×10^4	6.5×10^3
B	10^{20}	30.0	60.0				
C	10^{20}	100.0	200.0				
D	10^{22}	10.0	20.0	10^{-1}	.5		
E	10^{22}	30.0	60.0	2×10^{-2}	.2	1.78×10^3	8.0×10^2
F	10^{22}	100.0	200.0	3×10^{-3}	.05	7.50×10^3	2.7×10^3
					.05	2.63×10^3	1.1×10^2
G	10^{24}	10.0	20.0	10	2.3	7.7×10^1	2.7×10^1
H	10^{24}	30.0	60.0	2	.8	1.09×10^2	2.8×10^1
I	10^{24}	100.0	200.0	3×10^{-1}	.23	1.59×10^2	4.9×10^1
J	10^{24}	300.0	600.0	6×10^{-2}	.1	4.17×10^2	8.0×10^1
K	1.61×10^{24}	29.9	78.6	3	.9	7.82×10^1	5.3
L	1.61×10^{24}	91.47	12.1	6×10^{-1}	2.3	1.25×10^2	3.49

TABLE I: Initial density, temperature and plasma properties of the MD simulations

are found to be insensitive to small differences in the temperature parameters in (7), and a time-independent potential better conserves the total energy of the system. We similarly explored the sensitivity to other potential forms [17]. The results typically change by 10-15%, show no systematic trends, and are generally within the statistical error bars of one another.

We performed simulations for 12 different sets of initial conditions, two of which are equivalent to the cases considered by HM. In all cases, a pure hydrogen plasma is simulated using the true electron-proton mass ratio of 1:1836. A range of initial conditions span the weakly to strongly coupled regimes. Density and temperature variations chosen span the degenerate to non-degenerate regimes. Cases E, F, and I have degenerate electrons. The GMS-T and BPS theories along with the MD simulations do not take into account degeneracy effects and hence comparisons between theory and simulation are questionable. Table 1 lists the set of initial conditions considered for this study along with the electron degeneracy ($n_e\Lambda^3$) and H-plasma coupling ($\Gamma = e^2/R_{ion}kT$) parameters. The electron-proton relaxation time τ_{pe}^{sim} calculated by the code along with the error σ (standard deviation) are quoted in femtoseconds. Also included are two sets of initial conditions considered by HM.

III. COMPARISON WITH THEORY

In order to make comparisons with theoretical predictions easier, we define a simulation prediction for \mathcal{L} defined as $\mathcal{L}^{sim} = J_{LS}/\tau_{pe}^{sim}$. This result is then compared with the theoretical prediction for \mathcal{L} coming from GMS-T and BPS. Figure 1 shows simulation results for \mathcal{L}^{sim} with error bars and theoretical predictions for \mathcal{L}_{GMS} (solid) and \mathcal{L}_{BPS} (dashed) as a function of initial electron temperature. Numerical results and analytic expressions for

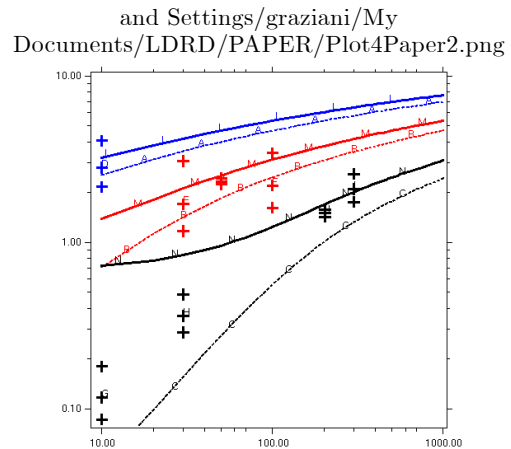


FIG. 1: Theoretical (GMS-T [solid] and BPS [dashed]) and MD calculations of \mathcal{L} as a function of initial T_e for densities $10^{20}/cc$, $10^{22}/cc$, and $10^{24}/cc$ (blue, red and black respectively). Additional detail is in the text.

\mathcal{L} are arranged according to density; $n = 10^{20}$, 10^{22} , and 10^{24} (blue, red and black respectively). The lowest density, highest temperature case is specially marked with a filled light blue circle. It was the only simulation run with a like charge system. That is, positron-proton. Degeneracy is not treated properly in either the simulations or the theories we consider. The points that have $n\Lambda^3 \gtrsim 1$ are denoted by an unfilled marker. They are shown for completeness but otherwise will not be discussed.

For plasmas with $\mathcal{L} > 1$, the simulation results are consistent with both the BPS and GMS-T forms of the Coulomb logarithm. It is not too surprising that both forms of \mathcal{L} would agree in the weakly coupled limit where $\mathcal{L} \gg 1$. What is interesting is that both forms do equally well at plasma conditions where \mathcal{L} is relatively small (i.e. $\mathcal{L} \sim 1$). For the high-density (10^{24}) cases where $\mathcal{L}^{sim} \lesssim 1$, the MD calculations are consistent with the GMS-T calculations and show a similar downward trend as T_e decreases. There is a slight downward systematic shift between GMS-T and the non-degenerate $n = 10^{24}$ MD results. However, the rather simple form of the effective Coulomb logarithm proposed by GMS does well over a wide range of plasma conditions. As expected, the BPS theory eventually becomes unstable at lower temperature when $n = 10^{24}$.

What does this discussion say about the LS model being accurate for $\mathcal{L}_{LS} \gtrsim 10$? Li and Petrasso [18] and GMS [7] argued that, for temperature equilibration, the restriction is $\mathcal{L}_{LS} \gtrsim 2$. The MD simulations offer an alternative approach that confirms this hypothesis. If one shifts the BPS curves downward, by the amount of the sub-leading correction (.679), it is seen that the LS theory is consistent with the numerical results provided $\mathcal{L}_{LS} \gtrsim 2$.

Ignoring degeneracy, is there an explanation for the systematic shift between simulations and \mathcal{L}_{GMS} at higher

temperatures for the high-density (10^{24}) cases? As stated above, \mathcal{L}_{GMS} comes from a T-matrix evaluation of the collision operator where it is assumed the screening is static. Given the good agreement between GMS-T and the MD results, a sense of the importance of dynamic screening effects can be assessed. The paper of GMS discusses a "combined model" which contains dynamical screening. The effect of this model occurs only at high density and it makes the electron-ion equilibration more rapid. When dynamical effects are allowed, the screening is weaker, the interaction stronger and the exchange rate faster. Since the rate is proportional to \mathcal{L} , the T-matrix result should be too low at high density. Dynamical corrections increase the effective \mathcal{L}^{sim} . Although not a proof, the systematic shift could be evidence of dynamical screening effects.

The paper of HM compared MD simulations to \mathcal{L}_{LS} . Even though our MD results for temperature equilibration are consistent with HM, our conclusions are different. \mathcal{L}_{LS} does not agree with the simulation results unless $\mathcal{L}_{LS} \gtrsim 2$ whereas the HM cases considered here have $\mathcal{L}^{sim} \lesssim 1$. In addition, case K starts out degenerate which neither theory or simulation treat correctly. The discrepancy between our conclusions and HM's can be traced to the fact that the HM definition of the relaxation rate is actually twice the relaxation rate defined by equation [1].

IV. CONCLUSIONS

We have performed large scale (10^5 electrons and ions) particle simulations of temperature equilibration for strongly and weakly coupled plasmas. For the weakly coupled plasmas where $\mathcal{L} \gtrsim 1$, the simulations agree

with both the Brown-Preston-Singleton and the fit to the T-matrix evaluation due to Gericke-Murillo-Schlanges. This agreement is a validation of our calculations. For plasmas with $\mathcal{L} \sim 1$, the importance of the sub-leading contributions of BPS become clear especially when comparing to MD results. For more strongly-coupled plasmas where $\mathcal{L} \lesssim 1$, we find that our simulations are consistent with the Gericke-Murillo-Schlanges theory. In fact, it is somewhat surprising that the rather simple form of effective Coulomb logarithm \mathcal{L}_{GMS} does so well over a wide range of plasma conditions. The major differences between Gericke-Murillo-Schlanges and the MD simulations typically occur where degeneracy is a factor. Our results are generally consistent with Hansen-McDonald, while having much higher numerical accuracy (500X the number of particles and 1/5 the time step). However, our conclusions are different. For the HM cases considered here, $\mathcal{L}_{LS} = \ln \lambda_D / \Lambda$ is not consistent with the MD results.

Looking towards the future, the simulations can be used to prepare tables of Coulomb logarithms for various density-temperature conditions (that work is underway). Finally, the simulations can now be extended by adding high Z impurities, superthermal particles (such as fusion alphas) and emission and absorption of radiation to provide a first-principles micro-physics simulation of thermonuclear burn.

V. ACKNOWLEDGMENTS

This work performed under the auspices of the U.S. Department of Energy by Lawrence Livermore National Laboratory under Contract DE-AC52-07NA27344.

-
- [1] P. Celliers, A. Ng, G. Xu, and A. Forsman, *Phys. Lett* **68**, 2305 (1992); A. Ng, P. Celliers, G. Xu, and A. Forsman, *Phys. Rev E* **52**, 4299 (1995).
 - [2] L. D. Landau, *Phys. Z. Sowjetunion* **10**, 154 (1936); *Sov. Phys. JETP* **7**, 203 (1937).
 - [3] L. Spitzer, Jr., *Physics of Fully Ionized Gases*, 2nd ed. (Interscience, New York, 1962).
 - [4] Y. T. Lee and R. M. More, *Phys. Fluids* **27**, 1273 (1984); J. D. Jackson, *Classical Electrodynamics* (Wiley, New York, 1975); R. Cauble and W. Rozmus, *Phys. Rev E* **52**, 2974 (1995).
 - [5] E. A. Frieman and D. C. Book, *Phys. Fluids* **6**, 1700 (1963).
 - [6] H. A. Gould and H. E. DeWitt, *Phys. Rev* **155**, 68 (1967).
 - [7] D. O. Gericke, M. S. Murillo, and M. Schlanges, *Phys. Rev. E* **65**, 036418 (2002).
 - [8] L. S. Brown, D. L. Preston, and R. L. Singleton, Jr., *Phys. Rep.* **410**, 237 (2005).
 - [9] L. S. Brown and R. L. Singleton, Jr., *Phys. Rev. E* **76**, 066404 (2007).
 - [10] J. P. Hansen and I. R. McDonald, *Phys. Lett.* **97A**, 42 (1983).
 - [11] F. H. Streitz, J. N. Glosli, and M. V. Patel, *Phys. Lett.* **96**, 225701 (2006).
 - [12] L. Greengard and V. Rokhlin, *J. Comp. Phys.* **73**, 325 (1987).
 - [13] D. O. Gericke and M. S. Murillo, *Inertial Fusion Sciences and Applications* **2003**; 1002 (2004).
 - [14] C. S. Jones and M. S. Murillo, *High Energy Density Physics* **3**, 379 (2007).
 - [15] T. Dunn and A. A. Broyles, *Phys. Rev.* **157**, 156 (1967).
 - [16] H. Minoo, M. M. Gombert and C. Deutsch, *Phys. Rev A* **24**, 1544 (1981).
 - [17] G. Kelbg, *Ann. Phys.* **12**, 219 (1963).
 - [18] C.-K. Li and R. D. Petrasso, *Phys. Rev. Lett.* **70**, 3059 (1993).